

The role of interactions, tunneling, and harmonic confinement on the adiabatic loading of bosons in an optical lattice

Ana Maria Rey,^{1,2,*} Guido Pupillo,^{1,3} and J. V. Porto¹

¹*National Institute of Standards and Technology, Gaithersburg, Maryland 20899, USA*

²*Institute for Theoretical Atomic, Molecular and Optical Physics, Harvard-Smithsonian Center of Astrophysics, Cambridge, Maryland 02138, USA*

³*Institute for Quantum Optics and Quantum Information of the Austrian Academy of Sciences, 6020 Innsbruck, Austria*

(Received 24 October 2005; revised manuscript received 14 December 2005; published 10 February 2006)

We calculate entropy-temperature curves for interacting bosons in unit filled optical lattices for both homogeneous and harmonically trapped situations, and use them to understand how adiabatic changes in the lattice depth affect the temperature of the system. In a translationally invariant lattice, the zero tunneling limit facilitates a rather detailed analytic description. Unlike the noninteracting bosonic system which is always cooled upon adiabatic loading for low enough initial temperature, the change in the excitation spectrum induced by interactions can lead to heating. Finite tunneling helps to reduce this heating. Finally, we study the spatially inhomogeneous system confined in a parabolic potential and show that the presence of the trap can significantly reduce the final available temperature, due to the nonvanishing superfluid component at the edge of the cloud which is present in trapped systems.

DOI: [10.1103/PhysRevA.73.023608](https://doi.org/10.1103/PhysRevA.73.023608)

PACS number(s): 03.75.Hh, 05.70.-a

I. INTRODUCTION

Cold atoms in optical lattices provide a system for realizing interacting many-body systems in essentially defect free lattices [1], and have been an active area of research in recent years. The strong interest in this system is due in part to the ability to dynamically control lattice parameters at a level unavailable in more traditional condensed matter systems. Lattice-based systems are typically governed by three sets of energy scales: interaction energies U , tunneling rates J , and the temperature T . In atomic systems, the energies U and J can be controlled by adjusting the lattice, and their values can be measured and/or calculated easily. Unlike condensed matter systems, however, it is experimentally difficult to measure very low temperatures ($kT < J$, $kT \leq U$, here k is the Boltzmann constant), and the temperature has so far only been inferred in a few cases [2–6]. Absent good thermometers, and given the ability to dynamically change the density of states, it is important to understand the thermodynamics of experimentally realistic systems in order to estimate the temperature.

It has been pointed out that loading sufficiently cold, noninteracting atoms into an optical lattice can lead to adiabatic cooling [7,8], but the cooling available in a real system will clearly depend on and be limited by interactions. It can also depend on the (typically harmonic) trapping potential, which provides an additional energy in the problem, as well as on the finite size of the sample. Here, we calculate the entropy of bosons in unit filled optical lattices for homogeneous and trapped cases. We provide good approximate, analytical expressions for the entropy for various cases, including finite number effects which allow for comparison of temperatures for adiabatic changes in the lattice.

For translationally invariant lattices at commensurate filling, the reduced density of states associated with the gap that appears in the insulating state presents a significant limitation to the final temperature when raising the lattice [3]. The presence of the trap, and the associated superfluidlike component at the edges can significantly increase the density of states, however, allowing for lower final temperatures.

In this paper we make the assumption of adiabatic loading and thus calculate the lowest possible final temperature achievable from a given initial temperature during the loading process. We realize that to be fully adiabatic might be experimentally challenging, however, our calculations could be used to benchmark the effect of the loading on the temperature of the atomic sample.

The paper is organized as follows. We start by introducing the model Hamiltonian and our notation. In Sec. III we focus on the translationally invariant case. We first develop analytic expression for the thermodynamic quantities in the $J=0$ limit and then we use them to calculate the final temperature of the atomic sample assuming we start with a dilute weakly interacting BEC, described using the Bogoliubov approximation. Next we study how finite size effects and finite J corrections modify the final temperature of the sample. In Sec. IV we discuss the effects of a spatial inhomogeneity induced by an additional parabolic potential and finally in Sec. V we conclude.

II. BOSE-HUBBARD HAMILTONIAN

The Bose-Hubbard (BH) Hamiltonian describes interacting bosons in a periodic lattice potential when the lattice is loaded such that only the lowest vibrational level of each lattice site is occupied and tunneling occurs only between nearest neighbors [1]

*Electronic address: arey@cfa.harvard.edu

$$H = - \sum_{\langle i,j \rangle} J_{ij} \hat{a}_i^\dagger \hat{a}_j + \frac{U}{2} \sum_j \hat{n}_j (\hat{n}_j - 1) + V_j \hat{n}_j. \quad (1)$$

Here \hat{a}_j is the bosonic annihilation operator of a particle at site $\mathbf{j} = \{j_x, j_y, j_z\}$, $\hat{n}_j = \hat{a}_j^\dagger \hat{a}_j$, and the sum $\langle i,j \rangle$ is over nearest neighbor sites. U is the interaction energy cost for having two atoms at the same lattice site which is proportional to the scattering length a_s , V_j accounts for any other external potential such as the parabolic magnetic confinement present in most of the experiments and J_{ij} is the hopping matrix element between nearest neighboring lattice sites.

For sinusoidal separable lattice potentials with depths $\{V_x, V_y, V_z\}$ in the different directions, the nearest-neighbor hopping matrix elements $\{J_x, J_y, J_z\}$ decrease exponentially with the lattice depth in the respective direction and U increases as a power law: $U \propto a_s (V_x V_y V_z)^{1/4}$ [1].

III. HOMOGENEOUS LATTICE

A. Thermodynamic properties in the $J=0$ limit

In this section we calculate expressions for the thermodynamic properties of N strongly correlated bosons in a spatially homogeneous lattice ($V_i=0$), with M sites. For the case where $J_{x,y,z}=0$, (relevant for very deep lattices) the entropy can be calculated from a straightforward accounting of occupation of Fock states, and is independent of the number of spatial dimensions. We derive expressions for the entropy per particle as a function of M, N, U and the temperature T , in the thermodynamic limit where $N \rightarrow \infty$ and $M \rightarrow \infty$, while the filling factor N/M remains constant.

In the $J_{x,y,z}=0$ limit, Fock number states are eigenstates of the Hamiltonian and the partition function \mathcal{Z} can be written as

$$\mathcal{Z}(N, M) = \sum_{\{n_r\}} \Omega(n_r) e^{-\beta \sum_r E_r n_r}, \quad (2)$$

where $\beta = (kT)^{-1}$, k is the Boltzmann constant. Here we use the following notation:

The quantum numbers n_r give the number of wells with r atoms, $r=0, 1, \dots, N$, in a particular Fock state of the system. For example for a unit filled lattice the state $|1, 1, \dots, 1, 1\rangle$ has quantum numbers $n_1=N$ and $n_{r \neq 1}=0$.

$$E_r \equiv U/2r(r-1).$$

The sum is over all different configurations $\{n_r\}$ which satisfy the constrains of having N atoms in M wells:

$$\sum_{r=0} n_r = M, \quad (3)$$

$$\sum_{r=0} r n_r = N. \quad (4)$$

$\Omega(n_r)$ accounts for the number of Fock states which have the same quantum numbers n_r and thus are degenerate due to the translational invariance of the system

$$\Omega(n_r) = \binom{M}{n_0, n_1, \dots, n_N} = \frac{M!}{n_0! n_1! \dots}. \quad (5)$$

Notice that without the particle number constraint, Eq. (4) and Eq. (2) could be easily evaluated. It would just be given by

$$\begin{aligned} \sum_N \mathcal{Z}(M) &= \sum_{n_0, n_1, \dots} \frac{M!}{n_0! n_1! \dots} (e^{-\beta E_0})^{n_0} (e^{-\beta E_1})^{n_1} \dots \\ &= \left(\sum_r e^{-\beta E_r} \right)^M. \end{aligned} \quad (6)$$

However, the constraint of having exactly N atoms, Eq. (4), introduces some complication. To evaluate the constrained sum we follow the standard procedure and go from a Canonical to a grandcanonical formulation of the problem.

Defining the grandcanonical partition function

$$\Xi(M) \equiv \sum_{N'} \mathcal{Z}(N', M) e^{\beta \mu N'} = \left(\sum_r e^{-\beta(E_r - \mu r)} \right)^M, \quad (7)$$

and using the fact that $\Xi(M)$ is a very sharply peaked function, the sum in Eq. (7) can be evaluated as the maximum value of the summand multiplied by a width ΔN^* :

$$\Xi(M) \approx \mathcal{Z}(N, M) e^{\beta \mu N} \Delta N^*. \quad (8)$$

Taking the logarithm of the above equation and neglecting the term $\ln(\Delta N^*)$, which in the thermodynamic limit is very small compared to the others ($\Delta N^* \ll N$), one gets an excellent approximation for the desired partition function $\mathcal{Z}(N'=N, M)$:

$$\ln[\mathcal{Z}(N, M)] = -\beta \mu N + \ln[\Xi(M)]. \quad (9)$$

The parameter μ has to be chosen to maximize $\mathcal{Z}(N', M) e^{\beta \mu N'}$ at N . This leads to the constraint

$$g = \sum_r r \bar{n}_r, \quad (10)$$

$$\bar{n}_r = \sum_s r \frac{e^{-\beta(E_r - \mu r)}}{\sum_s e^{-\beta(E_s - \mu s)}}, \quad (11)$$

where $g=N/M$ is the filling factor of the lattice, \bar{n}_r is the mean density of lattice sites with r atoms, and μ is the chemical potential of the gas.

From Eqs. (11) and (7) one can calculate all the thermodynamic properties of the system. In particular, the entropy per particle of the system can be expressed as

$$S(M, N) = k \left(-\beta \mu + \frac{1}{N} \ln[\Xi(M)] + \beta E \right), \quad (12)$$

where $E = (1/N) \sum_r E_r \bar{n}_r$ is the mean energy per particle.

1. Unit filled lattice $M=N$

For the case $M=N$ it is possible to show that, to an excellent approximation, the solution of Eq. (11) is given by

$$\mu = \frac{U}{2} - \ln[2] \frac{e^{-C\beta U}}{\beta}, \quad (13)$$

with $C=1.432$. Using this value of μ in the grandcanonical partition function one can evaluate all the thermodynamic quantities.

Low-temperature limit ($kT < U$). In the low-temperature regime $\mu \approx U/2$. By replacing $\mu = U/2$ in Eq. (7) one can write an analytic expression for Ξ and E (and thus for S) in terms of elliptic Theta functions [9] $\vartheta_3(z, q) = 1 + 2\sum_{n=1}^{\infty} q^{n^2} \cos[2nz]$:

$$\Xi(N) = \left[1 + \frac{e^{\beta U/2}}{2} [1 + \vartheta_3(0, e^{-\beta U/2})] \right]^N, \quad (14)$$

$$E = \frac{U}{2} \left[\frac{2 + \vartheta_3'(0, e^{-\beta U/2})}{2 + e^{\beta U/2} [1 + \vartheta_3(0, e^{-\beta U/2})]} \right], \quad (15)$$

with $\vartheta_3'(z, q) \equiv \partial \vartheta_3(z, q) / \partial q$. In this low-temperature regime one can also write an analytic expression for \bar{n}_r ,

$$\bar{n}_r = \left\{ \frac{2e^{-\beta U/2(r-1)^2}}{2 + e^{\beta U/2} [1 + \vartheta_3(0, e^{-\beta U/2})]} \right\}. \quad (16)$$

High-temperature limit ($kT > U$). In the high-temperature regime $\beta\mu \approx -\ln[(1+g)/g]$ which is just $\beta\mu = -\ln 2$ for the unit filled case. This can be easily checked by setting $\beta=0$ in Eq. (11) and solving for μ .

For large temperatures $\beta \rightarrow 0$, the grandcanonical partition function and the energy approach an asymptotic value $\ln[\Xi(M)] \rightarrow M[\ln(1+g)]$, $E \rightarrow Ug$. Therefore the entropy per particle reaches an asymptotic plateau $S/k \rightarrow (1/N) \ln[(1+g)^{N+M}/g^N] \approx \ln[\Omega_0]/N$. This plateau can be understood because $\Omega_0 = (N+M-1)!/(M-1)!N!$ is the number of all the possible accessible states to the system in the one-band approximation (total number of distinct ways to place N bosons in M wells). It is important to emphasize, however, that the one-band approximation is only valid for $kT \ll E_{\text{gap}}$, where E_{gap} is the energy gap to the second band. For example, for the case of ^{87}Rb atoms trapped in a cubic lattice potential $V_x = V_y = V_z$, $E_{\text{gap}} \geq 10U$ for lattice depths $V_x \geq 2E_R$. Here, E_R is the recoil energy, and $E_R = \hbar^2/(8md^2)$ where d is the lattice constant and m the atoms' mass. At higher temperatures the second band starts to become populated and thus the model breaks down.

In Fig. 1 we plot the entropy per particle as a function of temperature for a unit filled lattice. The (red) dash-dotted line corresponds to the numerical solution of Eqs. (7) and (11). The solid line (barely distinguishable from the numerical solution) corresponds to entropy calculated using the analytic expression of μ given in Eq. (13). The (blue) dashed line corresponds to the analytic expression of the entropy derived for the low-temperature regime in terms of elliptic Theta functions (14) and (15). From the plots one can see that Eq. (13) is a very good approximation for the chemical potential. Also the analytic expression derived for the low temperature regime reproduces well the numerical solution for temperatures $kT < U$.

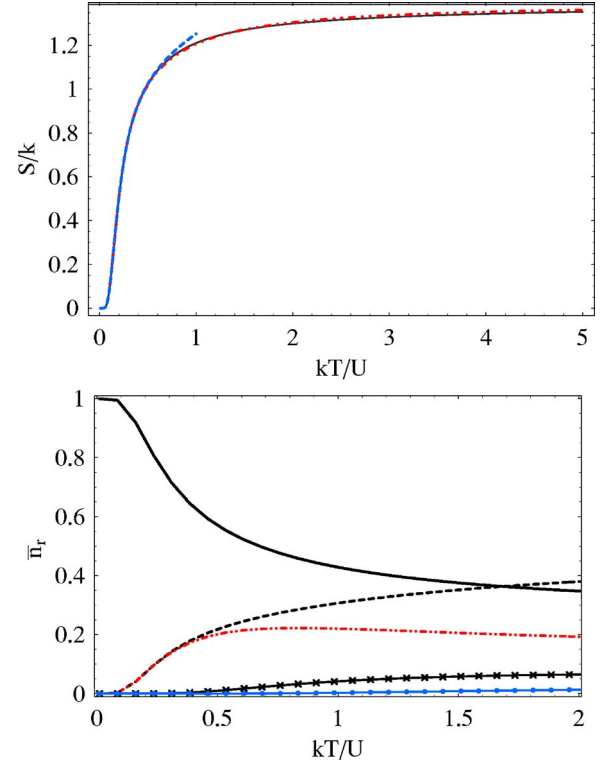


FIG. 1. (Color online) Top: Entropy per particle as a function of the temperature T (in units of U) for a unit filled lattice in the $J=0$ limit. Dash-dotted (red) line: Eq. (12) calculated using the numerical solution of Eqs. (7) and (11). Solid (black) line: entropy calculated using Eq. (13) for the chemical potential. Dashed (blue) line: Eq. (12) calculated using the low-temperature analytic solutions: Eqs. (14) and (15). Bottom: Average occupation number \bar{n}_r as a function of T (in units of U). The conventions used are \bar{n}_1 (continuous line), \bar{n}_0 (dashed), \bar{n}_2 (dotted-dashed), \bar{n}_3 (crosses), and \bar{n}_4 (dots).

It is also interesting to note the plateau in the entropy observed at extremely low temperatures, $kT < 0.05U$. This plateau is induced by the gapped excitation spectrum characteristic of an insulator which exponentially suppresses the population of excited states at very low temperatures. As we will discuss below the range of temperature over which the plateau exists is reduced if J is taken into account.

In Fig. 1 we also show \bar{n}_r , the average densities of sites with r atoms vs temperature calculated using Eqs. (13) and (11). In particular \bar{n}_1 is important because lattice based quantum information proposals [10–12] rely on having exactly one atom per site to initialize the quantum register and population of states with $r \neq 1$ degrades the fidelity. Specifically we plot \bar{n}_1 (solid line), \bar{n}_0 (dashed line), \bar{n}_2 (dotted-dashed), \bar{n}_3 (crosses), and \bar{n}_4 (points).

In the entropy-plateau region of Fig. 1, corresponding to $kT < 0.05U$, particle-hole excitations are exponentially inhibited and thus \bar{n}_1 is almost 1. For temperatures $kT < U/2$, \bar{n}_0 is almost equal to \bar{n}_2 , meaning that only particle-hole excitations are important. As the temperature increases, $kT > U/2$, states with three atoms per well start to become populated and therefore \bar{n}_0 becomes greater than \bar{n}_2 . The population of states with $r \geq 3$ explains the break down of the analytic

solution written in terms of elliptic functions for $kT > U/2$ as this solution assumes $\bar{n}_0 = \bar{n}_2$. For $kT > 2U$, even states with 4 atoms per well become populated and the fidelity of having unit filled wells degrades to less than 60%.

B. Adiabatic loading

In this section we use the entropy curves derived in the previous section for the unit filled lattice to calculate how the temperature of a dilute 3D Bose-Einstein condensate (BEC) changes as it is adiabatically loaded into a deep optical lattice. Ideally the adiabatic loading process will transfer a $T=0$ BEC into a perfect Mott Insulator (MI), however, condensates cannot be created at $T_i=0$ and it is important to know the relation between final and initial temperatures. Calculations for an ideal bosonic gas [7] demonstrate that for typical temperatures at which a BEC is created in the laboratory, adiabatically ramping up the lattice has the desirable effect of cooling the system. On the other hand, drastic changes in the energy spectrum (the opening up of a gap) induced by interactions modify this ideal situation [3] and in the interacting case atoms can be instead heated during the loading.

In order to calculate the change in the temperature due to the loading, we first calculate the entropy as a function of temperature of a dilute uniform BEC of ^{87}Rb atoms by using Bogoliubov theory. The Bogoliubov approximation is good for a dilute gas as it assumes that quantum fluctuations introduced by interactions are small and treats them as a perturbation. The quartic term in the interacting many-body Hamiltonian is approximated by a quadratic one which can be exactly diagonalized [13,14]. This procedure yields a quasi-particle excitation spectrum given by $\epsilon_{\mathbf{p}} = \sqrt{(\epsilon_{\mathbf{p}}^0)^2 + 2un\epsilon_{\mathbf{p}}^0}$. Here $\epsilon_{\mathbf{p}}^0 = \mathbf{p}^2/2m$ are single particle energies, $u = 4\pi\hbar^2 a_s/m$, m is the atomic mass, and n is the gas density.

Using this quasiparticle spectrum in the Bose distribution function of the excited states, $f(\epsilon_{\mathbf{p}}) = [e^{\beta\epsilon_{\mathbf{p}}} - 1]^{-1}$, one can evaluate the entropy of the gas given by

$$S|_{V_{x,y,z}=0} = k \sum_{\mathbf{p}} \{ \beta \epsilon_{\mathbf{p}} f(\epsilon_{\mathbf{p}}) - \ln[1 - e^{-\beta\epsilon_{\mathbf{p}}}] \}. \quad (17)$$

Using Eq. (17) we numerically calculate the entropy of the system for a given initial temperature T_i . Assuming the entropy during the adiabatic process is kept constant, to evaluate T_f for a given T_i we solve the equation

$$S(T_i)|_{V_{x,y,z}=0} = S(T_f)|_{V_{x,y,z}=V_f}. \quad (18)$$

We evaluate the right hand side of this equality assuming that the final lattice depth V_f is large enough that we can neglect terms proportional to J in the Hamiltonian. We use the expression for the entropy derived in the previous section, Eq. (12), together with Eqs. (14) and (15).

The results of these calculations are shown in Fig. 2, where we plot T_f vs T_i for three different final lattice depths $V_f/E_R = 10$ (dashed line), 20 (dot-dashed line), and 30 (long-dashed line). In the plot both T_f and T_i are given in recoil units E_R . As a reference, the critical BEC temperature for an ideal bosonic gas (which for a dilute gas is only slightly

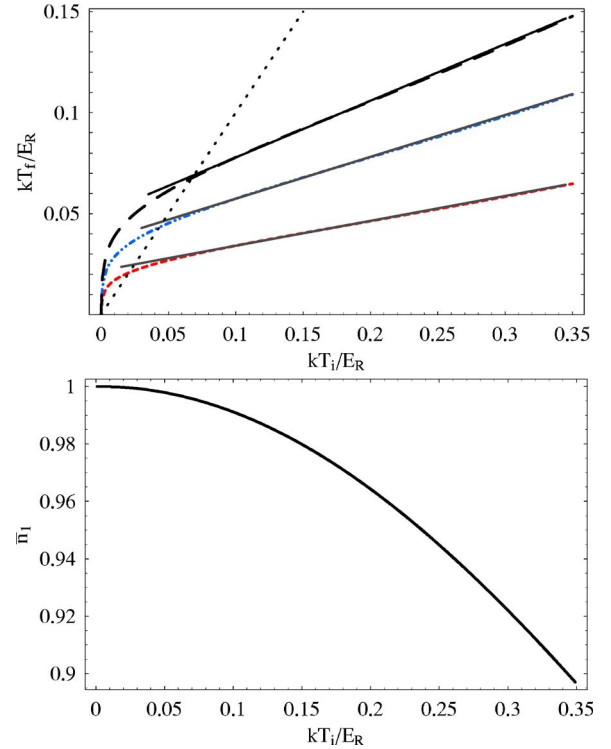


FIG. 2. (Color online) Top: T_f vs T_i (in units of E_R) for different final lattice depths V_f . Here, we assume adiabatic loading in the limit $J=0$. The dashed (red), dot-dashed (blue), and long-dashed (black) lines are for $V_f=10, 20$, and $30E_R$, respectively. The continuous (grey) lines are calculated for the various lattice depths from Eq. (19). The dotted line is the identity $T_f=T_i$. Bottom: Average density of unit filled cells \bar{n}_1 as a function of T_i (in units of E_R).

affected by interactions) in recoil units is $kT_c^0 \approx 0.67E_R$.

For $kT_i > 0.05E_R$ the final temperature scales linearly with T_i :

$$kT_f = \frac{U}{3E_R}(kT_i + 0.177E_R). \quad (19)$$

In Fig. 2, Eq. (19) is plotted with a gray line for the various final lattice depths.

In contrast to the noninteracting case, where for $kT_i < 0.5E_R$ the system is always cooled when loading into the lattice [7], here interactions can heat the atomic sample for low enough initial temperatures. For reference in Fig. 2, we show the line $T_f=T_i$. One finds a temperature $T^{\text{heat}}(V_f)$ (determined from the intersection of the $T_f=T_i$ line with the other curves) below which the system heats upon loading into a lattice of depth V_f . From the linear approximation one finds that T^{heat} increases with U as $kT^{\text{heat}}(V_f) \approx 0.177U(3 - U/E_R)^{-1}$. Because U scales as a power law with the lattice depth [1], a larger V_f implies a larger $T^{\text{heat}}(V_f)$ and so a larger heating region. Note that for the shallowest lattice in consideration, $V_f/E_R = 10$, $kT^{\text{heat}} < 0.05$ and therefore the linear approximation does not estimate it accurately. Figure 2 also shows a very rapid increase in the temperature close to $T_i=0$. This drastic increase is due to the low temperature plateau induced by the gap that opens in the insulating phase.

To quantify the particle-hole excitations and give an idea of how far from the target ground state the system is after the loading process, we also plot \bar{n}_1 vs T_i in the bottom panel of Fig. 2. In the plot, \bar{n}_1 is calculated from Eq. (16). We found that to a very good approximation

$$\bar{n}_1(T_i) = \left[1 - \exp\left(\frac{-3}{2kT_i/E_R + 0.354}\right) \right]^{-1}. \quad (20)$$

Note that in the $J=0$ limit, \bar{n}_1 depends exclusively on βU and thus as long as the final lattice depth is large enough to make the $J=0$ approximation valid, \bar{n}_1 is independent of the final lattice depth. The exponential suppression of multiple occupied states in the entropy plateau explains why even though the final temperature increases rapidly near $T_i=0$, this is not reflected as a rapid decrease of \bar{n}_1 . For the largest initial temperature displayed in the plot $kT_i/E_R \approx T_c^0/2$, the final temperature reached in units of U is $kT_f/U \approx 0.17$ and $\bar{n}_1 \approx 0.9$. Thus, the fidelity of the target state has been degraded to less than 90%. In Fig. 1 one also observes that $\bar{n}_1 \approx 0.9$ at $kT_f/U \approx 0.17$ and that most of the loss of fidelity is due to particle-hole excitations as $\bar{n}_{r>3} \approx 0$.

C. Finite size effects

In recent experiments by loading a BEC into a tight two-dimensional optical lattice, an array of quasi-one-dimensional tubes has been created [2,15–18]. The number of atoms in each tube is of the order of less than 10^2 and therefore the assumption of being in the thermodynamic limit is no longer valid for these systems.

The thermodynamic limit assumption used in the previous section allowed us to derive thermodynamic properties without restricting the Hilbert space in consideration. Thus, within the one-band approximation, these expressions were valid for any temperature. However, if the size of the system is finite, number fluctuations ΔN must be included and to derive expressions valid for arbitrary temperatures could be difficult. In this section we calculate finite size corrections by restricting the temperature to $kT < U/2$. At such temperatures Fig. 1 shows that only states with at most two atoms per site are relevant so one can restrict the Hilbert space to include only states with at most two atoms per site.

Setting $\bar{n}_{r>2}=0$ and $M=N$ in Eq. (2), the partition function (at zero order in J) can be explicitly written as

$$\begin{aligned} \mathcal{Z}(N,N) &= \sum_{j=0}^{\lfloor N/2 \rfloor} \frac{N!}{(j!)^2(N-2j)!} e^{-\beta U j}, \\ &= e^{-\beta U/2} \cos(\pi N) C_N^{(-N)} \left[\frac{1}{2} e^{\beta U/2} \right], \end{aligned} \quad (21)$$

where $C_n^{(m)}[x]$ are Gegenbauer polynomials [9].

In Fig. 3 (left panel) we study the effect of finite atom number on the entropy. We show the entropy per particle as a function of temperature for systems with $N=50$ (green dotted line), $N=100$ (blue dashed line), and $N=1000$ (red dash-dotted line). For comparison purposes we also plot with a (black) solid line the entropy calculated using Eqs. (14) and (15), which were derived in the thermodynamic limit. It can

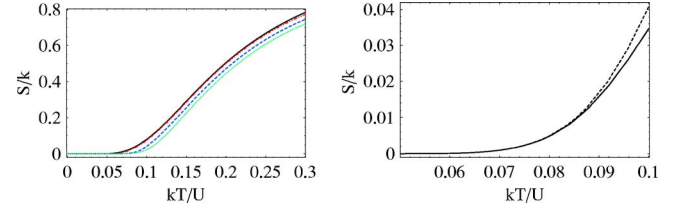


FIG. 3. (Color online) Left: Entropy per particle S as a function of the temperature T (in units of U) for a unit filled lattice in the $J=0$ limit and different number of atoms N . The solid line shows S calculated in the thermodynamic limit using Eqs. (14) and (15). The dash-dotted (red), dashed (blue), and dotted (green) lines correspond to $N=1000, 100$, and 50 , respectively. For these curves, S is restricted to the p-h subspace [see Eq. (21)]. Right: S vs T (in units of U) for $N=100$. The dashed and solid lines are the entropy calculated in the p-h and 1-p-h [see Eq. (22)] subspaces, respectively.

be observed that for $N=1000$ the thermodynamic limit is almost reached (nearly indistinguishable from the thermodynamic limit). Finite size effects decrease the entropy per particle and thus tend to increase the final temperature during the adiabatic loading.

Furthermore, in the right panel we also compare Eq. (21) with the entropy calculated by restricting the Hilbert space even more and including only one-particle-hole (1-p-h). 1-p-h excitations are the lowest lying excitations which correspond to states that have one site with two atoms, one with zero atoms and one atom in every other site, i.e., $\{n_r\}_U = \{1, N-2, 1, 0, \dots, 0\}$. There are $N(N-1)$ different particle hole excitations all with energy U . If the entropy is calculated taking into account only 1-p-h excitations one gets an expression to zeroth order in J given by

$$\frac{S}{k} \approx \frac{\ln[1 + N(N-1)e^{-\beta U}]}{N} + \frac{\beta U(N-1)e^{-\beta U}}{1 + N(N-1)e^{-\beta U}}. \quad (22)$$

The right panel shows that as long as the temperature is below $kT \ll 0.1U$ and the number of wells is of order 10^2 or less, Eq. (22) gives a very good approximation for the entropy per particle.

D. Finite J corrections

In the previous section for simplicity we worked out the thermodynamic quantities assuming $J=0$. However, if the final lattice is not deep enough, finite J corrections should be taken into account. In this section we study how these corrections can help to cool the unit filled lattice during adiabatic loading.

In the $J=0$ limit all thermodynamic quantities are independent of the dimensionality of the system. On the other hand, for finite J the dimensionality becomes important. Including J in the problem largely complicates the calculations as number Fock states are no longer eigenstates of the many-body Hamiltonian and many degeneracies are lifted. For simplicity, in our calculations we will focus on the 1D case and assume periodic boundary conditions. We will also limit our calculations to systems with less than 10^2 atoms and

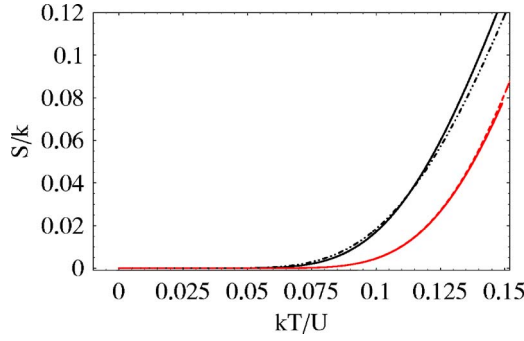


FIG. 4. (Color online) Finite J corrections: The dash-dotted and broken lines correspond to the entropy per particle vs T (in units of U) calculated by numerical diagonalizations of the Hamiltonian for systems with $N=10$ atoms and $J/U=0.1$ and 0.01 , respectively. The corresponding solid lines show the entropy per particle calculated from Eq. (24).

temperatures low enough ($kT \ll 0.1U$) so it is possible to restrict the Hilbert space to include only 1-p-h excitations.

To find first-order corrections to the $N(N-1)$ low lying excited states we must diagonalize the kinetic energy Hamiltonian within the 1-p-h subspace. For one-dimensional (1D) systems this diagonalization yields the following approximated expression for the eigenenergies [19]:

$$E_{rR}^{(1)} = U - 4J \cos\left(\frac{\pi r}{N}\right) \cos\left(\frac{\pi R}{N}\right), \quad (23)$$

where $r=1, \dots, N-1$ and $R=0, \dots, N-1$. Using these eigenenergies to evaluate the entropy per particle one obtains the following expression:

$$\frac{S}{k} \approx \frac{\ln Z}{N} + U\beta(N-1) \frac{\left[I_0^2(2J\beta) - \frac{4J}{U} I_0(2J\beta) I_1(2J\beta) \right]}{Z} e^{-\beta U},$$

with

$$Z = 1 + N(N-1)e^{-\beta U} I_0(2J\beta), \quad (24)$$

where $I_n(x)$ are modified Bessel functions of the first kind [9].

To derive Eq. (23), we assumed similar effective tunneling energies for the extra particle and the hole. This is not exact, especially for a unit filled lattice, $g=1$, since the effective hopping energy for the particles and holes goes as $J(g+1)$ and Jg , respectively. However, we find by comparisons with the exact diagonalization of the Hamiltonian that for observables such as the partition function which involves summing over all the 1-p-h excitations, this assumption compensates higher order corrections in J/U neglected to first order. It even gives a better expression for the entropy of the many-body system than the one calculated by using the spectrum obtained by exact diagonalization in the 1-p-h subspace.

We show the validity of Eq. (24) in Fig. 4 where we compare its predictions (plotted with solid lines) with the entropy calculated by exact diagonalization of the Bose-Hubbard Hamiltonian for different values of J/U assuming a

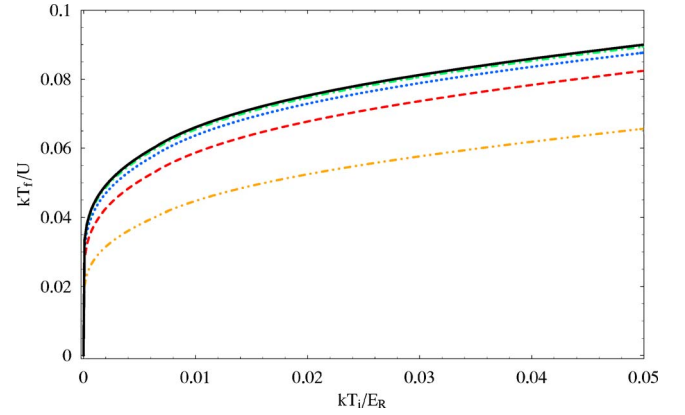


FIG. 5. (Color online) T_f (in units of U) vs T_i (in units of E_R) curves calculated using Eq. (24) for a system with $N=100$ atoms and different values of J/U : dash-dot-dotted (yellow) line $J/U=0.12$ ($V_z=5E_R$), dashed (red) line $J/U=0.07$ ($V_z=7E_R$), dotted (blue) line $J/U=0.04$ ($V_z=9E_R$) and dash-dotted (green) line $J/U=0.07$ ($V_z=11E_R$). The solid (black) lines is shown for comparison purposes and corresponds to the limiting case $J=0$.

system with $N=10$ atoms. In the plot we use a dot-dashed line for $J/U=0.1$ and a dashed line for $J/U=0.01$. Even for the case $J/U=0.1$ we see the analytic solution reproduces very well the exact solution, especially at low temperatures. At $kT > 0.11U$ higher order corrections is J/U become more important.

We now use Eq. (24) to study larger systems where an exact diagonalization is not possible. Even though we expect finite J corrections to become important at lower temperatures for larger systems, we consider that for systems with less than 10^2 atoms, small values of J/U and within the low-temperature restriction, Eq. (24) can still give a fair description of the entropy. In Fig. 5 we show the effect of finite J corrections on the final temperature of a system of 100 ^{87}Rb atoms when adiabatically loaded. For the calculations, we fix the transverse lattice confinement to $V_x=V_y=30E_R$, assume $d=405$ nm and vary the axial lattice depth. We show the cases $V_z=5E_R$ with a yellow dash-dot-dotted line, $V_z=7E_R$ with a red dashed line, $V_z=9E_R$ with blue dotted line, and $V_z=11E_R$ with a green dash-dotted line. For these lattice depths, the single-band approximation is always valid and the energies J and U both vary so that their ratio decreases as $J/U=\{0.12, 0.07, 0.04, 0.02\}$, respectively. We also plot for comparisons purposes the $J/U=0$ case with a solid black line.

Figure 5 shows that finite J corrections decrease the final available temperature of the sample. These corrections are important for shallower lattices, as they decrease the final temperature with respect to the $J=0$ case by about 30%. For lattices deeper than $V_z=11E_R$ the corrections are very small.

The decrease in the final temperature induced by J can be qualitatively understood in terms of the modifications that hopping makes to the eigenenergies of the system. J breaks the degeneracy in the 1-p-h, leading to a quasiband whose width is proportional to J . As J increases the energy of the lowest excited state decreases accordingly, while the ground state is only shifted by an amount proportional to J^2/U . The lowest energy excitations then lie closer to the ground state

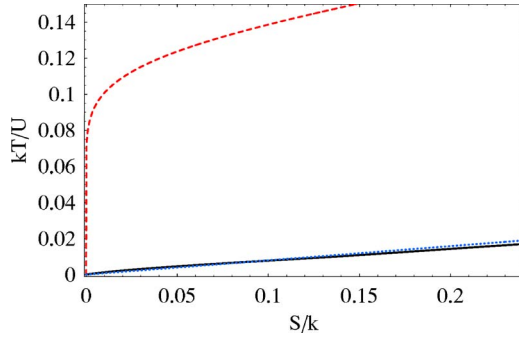


FIG. 6. (Color online) Final temperature (in units of U) vs initial entropy per particle. The solid (black) line corresponds to the trapped system with the parameters chosen to closely reproduce the experimental setup of Ref. [2]. The dotted (blue) line is the analytic solution for a system of fermions at low temperature assuming a boxlike spectrum and the dashed (red) line is the entropy for the correspondent homogeneous system calculated from Eq. (22).

and become accessible at lower temperatures. As a consequence, the entropy increases (and thus T_f decreases) with respect to the $J=0$ case.

Following the same lines of reasoning the entropy should exhibit a maximum at the critical point associated with the Mott insulator transition, since at this point an avoided crossing takes place. We confirmed this intuitive idea with exact numerical diagonalization of small systems. For the translationally invariant case, we expect the entropy to become sharply peaked at the transition with increasing N and this could be an important limitation for adiabatically loading atoms. However, as we will discuss later, the external harmonic confinement present in most experiment prevents a sharp Mott insulator transition and can help to decrease the adiabaticity loading time within accessible experimental time scales.

In this section we focused on the effect of finite J corrections in 1D systems. For higher dimensions, we expect that finite J corrections help to cool the system even more, since the effective tunneling rate that enters in the entropy scales with the number of nearest neighbors and thus becomes larger for higher dimensions.

IV. HARMONIC CONFINEMENT: $V_i = \Omega i^2$

For simplicity in our analysis we consider a 1D system which can be studied using standard fermionization techniques [20]. These techniques allow us to map the complex strongly correlated bosonic gas into a noninteracting fermionic one. We choose our parameters so that they closely resemble the experimental ones used in Ref. [2]. Specifically we use transverse lattice depths $V_x = V_y = 27E_R$ created by lasers with wavelength $\lambda_x = 823$ nm and an axial lattice depth of $V_z = 18.5E_R$ created by a laser of wavelength $\lambda_z = 854$ nm. We set the axial frequency of the 1D gas to $\omega_z = 2\pi \times 60$ Hz and the number of atoms to $N=19$ (this was the mean number of atoms in the central tube of the experiment). For these parameters the ratio $U/J \sim 205$ and $\Omega/J = 0.28$ with $\Omega \equiv 1/8m\omega_z^2\lambda_z^2$. The

ground state of the system corresponds to a MI with N unit filled sites at the trap center (see Fig. 7 bottom panel). We compare the thermodynamic properties of this system with the ones of a translationally invariant system in the MI state, with the same number of atoms ($N=M=19$) and same ratio U/J . As we described in the previous section, for homogeneous systems the finite J corrections for the $J/U \sim 0.005$ ratio in consideration are very small, and for temperatures below $kT/U \lesssim 0.1$ they can be neglected. On the contrary, when the parabolic confinement is present, taking into account the kinetic and trapping energy corrections is crucial for a proper description of the low temperature properties of the system. Unlike the spatially invariant case, where the lowest lying excitations in the MI phase are 1-p-h excitations which have an energy cost of order U , in the trapped case, within the parameter regime in consideration, there are always lower-lying excitations induced by atoms tunneling out from the central core and leaving holes inside it. We refer to these excitations as n -hole (n -h) excitations. These “surface” n -h excitations must be included in the trapped system because of the reservoir of empty sites surrounding the central core, which introduces an extra source of delocalization. For example the lowest lying hole excitations correspond to the 1-h excitations created when a hole tunnels into one of the most externally occupied sites. They have energy cost ΩN , which for the parameters in Ref. [2] is 40 times smaller than U .

For a system in arbitrary dimensions, it is complicated to properly include n -h excitations in the calculations of thermodynamic properties. For 1D systems, however, the Bose-Fermi mapping allows us to include them in a very simple way. Nevertheless, because fermionization techniques neglect multioccupied wells in the system we have to restrict the analysis to temperatures at which no multiple occupied states are populated ($kT \lesssim 0.1U$, see also Ref. [4]). The results are shown in Fig. 6, where we plot the final temperature of the sample as a function of a given initial entropy S . In the plot we also show the results for the corresponding translationally invariant system.

The most important observation is that instead of the sudden temperature increase at $S=0$ (or flat S vs T plateau induced by the gap), in the trapped case the temperature increases slowly and almost linearly with S :

$$S \approx A \left(\frac{T}{T_F} \right), \quad (25)$$

$$A = 5k \left(\frac{\pi}{6} \right)^2, \quad (26)$$

with T_F the Fermi temperature. The linear behavior is characteristic of low temperature degenerate Fermi gases and the proportionality constant A depends on the density of states of the system. For this particular case, A can be estimated assuming a boxlike dispersion spectrum $E_n = \Omega n^2$. For the parameter regime in consideration this assumption is valid for the modes close to the Fermi energy, which are the relevant ones at low temperature (Ref. [22]). Using this boxlike spectrum it is possible to show that for $\Omega < kT \ll kT_F$ (where the

first assumption allows a semiclassical approximation) A is given by Eq. (26). In Fig. 6 the blue-dotted line corresponds to this linear solution and it can be seen that it gives a fair description of the entropy in the low temperature regime. It is interesting to point out that the slower increase in entropy as a function of temperature in the homogeneous system compared to the trapped one is a particular effect induced by interactions. In the noninteracting case the opposite behavior is observed: for an homogeneous system $S^h \propto (T/T_c)^{D/2}$, whereas for the trapped system $S^\omega \propto (T/T_c)^D$ so if $T < T_c$ then $S^h > S^\omega$. Here D is the dimensionality of the system and T_c the critical condensation temperature.

In a typical experiment the sample is prepared by forming a BEC in a magnetic trap. Therefore a good estimate of the initial entropy is given by [21]

$$S = k \left(4\zeta(4)/\zeta(3)t^3 + \frac{1}{3}t^2(1-t^3)^{2/5} \right), \quad (27)$$

where $\eta = \alpha(N^{1/6}a_s/\bar{a}_{ho})^{2/5}$, with $\alpha = 15^{2/5}[\zeta(3)]^{1/3}/2 \approx 1.57$ and $\bar{a}_{ho} = \sqrt{\hbar/(m\bar{\omega})}$ the mean harmonic oscillator length ($\bar{\omega} = \sqrt[3]{\omega_x\omega_y\omega_z}$). The parameter η takes into account the main corrections to the entropy due to interactions. In the above equation $t = T/T_c$ with $T_c = T_c^0(1 - 0.43\eta^{5/2})$ the critical temperature for condensation and T_c^0 the critical temperature for the ideal trapped gas $kT_c^0 = \hbar\bar{\omega}[N/\zeta(3)]^{1/3}$. The term proportional to $\eta^{5/2}$ accounts for the small shift in the critical temperature induced by interactions. For typical experimental parameters η ranges from 0.35 to 0.4.

If one assumes a $N = 10^{5-6}$ atoms, $\bar{\omega}/(2\pi) = 60-120$ Hz and a very cool initial sample, $t \sim 0.2$, one obtains that in typical experiments the initial entropy per particle of the system is not smaller than $S/k \geq 0.1$. Figure 6 shows then that the reduction of the final temperature during the adiabatic loading induced by the trap can be significant. In turn, this suggests that the presence of the magnetic confinement is going to be crucial in the practical realization of schemes for lattice-based quantum computation.

To emphasize this point, in Fig. 7 (top panel) we plot the mean occupancy of some lattice sites as a function of the initial entropy per particle. It should be noted that for the number of atoms in consideration the edge of the cloud at $T=0$ is at $j = (N-1)/2 = 9$. For comparison purposes we also plot \bar{n}_1 calculated for the correspondent spatially homogeneous system. The plots shows that for the central lattice sites there is almost 100% fidelity to have one atom per site for the range of initial entropies in consideration. Fluctuations are only important at the edge of the cloud and if one excludes these extremal sites the fidelity in the trap case remains always higher than the fidelity in absence of the trap. In the bottom panel we also show the density profile for $S=0$ and compare it with the one at $S/k=0.25$. It is clear in the plot that the central lattice sites remain almost with one atom per site.

The considerations made here are for adiabatic changes to the lattice, and therefore represent a lower bound on the final temperature, assuming the entropy is fixed. How quickly the lattice can be changed and remain adiabatic is a separate issue, but we point out that for systems with finite number of

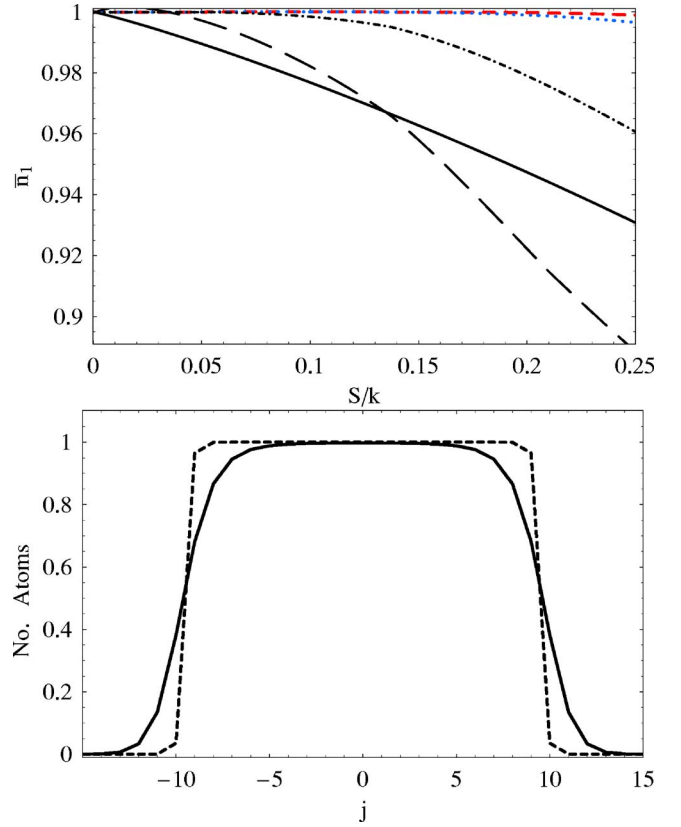


FIG. 7. (Color online) Top: Local on-site probability of having unit filling \bar{n}_1 as a function of the entropy per particle S , and for a few values of the site index j . The dashed (red), dotted (blue), dot-dashed (black), and long-dashed (black) lines correspond to the sites with $j=0, 4, 7$, and 8 , respectively. For comparison purposes, we also plot \bar{n}_1 calculated for the correspondent spatially homogeneous system (solid line). Bottom: Density profile for the trapped system in consideration at $S/k=0$ (dashed line) and $S/k=0.25$ (solid line).

atoms confined by an external trap there is not a sharp superfluid/insulator phase transition, which should relax the adiabaticity requirements when passing through the transition region. A proper adjustment of the harmonic confinement during the loading process could reduce the time scales required for adiabaticity to be experimentally realizable.

V. CONCLUSIONS

In this paper we calculated entropy-temperature curves for interacting bosons in unit filled optical lattices and we used them to understand how adiabatic changes in the lattice depth affect the temperature of the system. For the uniform system, we have derived analytic expressions for the thermodynamic quantities in the $J/U=0$ case and we used them to identify the regimes wherein adiabatically changing the lattice depth will cause heating or cooling of the atomic sample in the case of a unit filled lattice. We have shown that the heating is mainly induced by the gapped excitation spectrum characteristic of the insulator phase. By considering finite size effects and finite J corrections we have shown that the

former leads to increased the heating of the atoms, the latter tend to reduce it.

Finally, we have discussed the spatially inhomogeneous system confined in a parabolic potential and we have shown that the presence of the trap reduces significantly the final available temperature of the atoms due to the low-energy surface excitations always present in trapped systems. The fact that the harmonic confinement turns out to be clearly a desirable experimental tool for reducing temperature in the lattice is an important finding which should be taken into account in the ongoing experimental and theoretical efforts aimed at using the Mott Insulator transition as a means to initialize a register for neutral atom quantum computation.

Note added in proof. Recently we have learned of a report

by K. P. Schmidt *et al.* [23] which partially overlaps with our present work.

ACKNOWLEDGMENTS

This work was supported in part by the Advanced Research and Development Activity (ARDA) contract and the U.S. National Science Foundation through Grant No. PHY-0100767. A.M.R. acknowledges additional support by a grant from the Institute of Theoretical, Atomic, Molecular, and Optical Physics at Harvard University and Smithsonian Astrophysical observatory. G.P. acknowledges additional support from the European Commission through a Marie-Curie grant of the Optical Lattices and Quantum Information (OLAQUI) Project.

-
- [1] D. Jaksch, C. Bruder, J. I. Cirac, C. W. Gardiner, and P. Zoller, *Phys. Rev. Lett.* **81**, 3108 (1998).
- [2] B. Paredes, A. Widera, V. Murg, O. Mandel, S. Fölling, I. Cirac, G. V. Shlyapnikov, T. W. Hänsch, and I. Bloch, *Nature (London)* **429**, 277 (2004).
- [3] A. Reischl, K. P. Schmidt, and G. S. Uhrig, *Phys. Rev. A* **72**, 063609 (2005).
- [4] G. Pupillo, C. J. Williams, and Nikolay V. Prokof'ev, *Phys. Rev. A* **73**, 013408 (2006).
- [5] T. Stöferle, H. Moritz, K. Günter, M. Köhl, and T. Esslinger, *Phys. Rev. Lett.* **96**, 030401 (2006).
- [6] H. G. Katzgraber, A. Esposito, and M. Troyer, e-print cond-mat/0510194.
- [7] P. B. Blakie and J. V. Porto, *Phys. Rev. A* **69**, 013603 (2004); P. B. Blakie and A. Bezzet, *ibid.* **71**, 033616 (2005).
- [8] W. Hofstetter, J. I. Cirac, P. Zoller, E. Demler, and M. D. Lukin, *Phys. Rev. Lett.* **89**, 220407 (2002).
- [9] I. Abramowitz, and I. A. Stegun, *Handbook of Mathematical Functions* (National Bureau of Standards, Washington, D.C., 1964).
- [10] D. Jaksch, H.-J. Briegel, J. I. Cirac, C. W. Gardiner, and P. Zoller, *Phys. Rev. Lett.* **82**, 1975 (1999).
- [11] T. Calarco, H.-J. Briegel, D. Jaksch, J. I. Cirac, and P. Zoller, *J. Mod. Opt.* **47**, 2137 (2000).
- [12] G. Pupillo, A. M. Rey, G. K. Brennen, C. J. Williams, and C. W. Clark, *J. Mod. Opt.* **51**, 2395 (2004); G. K. Brennen, G. Pupillo, A. M. Rey, C. W. Clark, and C. J. Williams, *J. Phys. B* **38**, 1687 (2005).
- [13] K. Berg-Sørensen and K. Mølmer, *Phys. Rev. A* **58**, 1480 (1998).
- [14] K. Burnett, M. Edwards, C. W. Clark, and M. Shotton, *J. Phys. B* **35**, 1671 (2002).
- [15] B. L. Tolra, K. M. O'Hara, J. H. Huckans, W. D. Phillips, S. L. Rolston, and J. V. Porto, *Phys. Rev. Lett.* **92**, 190401 (2004).
- [16] H. Moritz, T. Stöferle, M. Köhl, and T. Esslinger, *Phys. Rev. Lett.* **91**, 250402 (2003).
- [17] T. Kinoshita, T. Wenger, and D. S. Weiss, *Science* **305**, 1125 (2004).
- [18] C. D. Fertig, K. M. O'Hara, J. H. Huckans, S. L. Rolston, W. D. Phillips, and J. V. Porto, *Phys. Rev. Lett.* **94**, 120403 (2005).
- [19] A. M. Rey, P. B. Blakie, G. Pupillo, and C. J. Williams, and C. W. Clark, *Phys. Rev. A* **72**, 023407 (2005).
- [20] M. Girardeau, *J. Math. Phys.* **1**, 516 (1960).
- [21] F. Dalfovo, S. Giorgini, L. P. Pitaevskii, and S. Stringari, *Rev. Mod. Phys.* **71**, 463 (1999).
- [22] A. M. Rey, G. Pupillo, C. W. Clark, and C. J. Williams, *Phys. Rev. A* **72**, 033616 (2005).
- [23] K. P. Schmidt, A. Reischl, and G. S. Uhrig, e-print cond-mat/0510461.